Identification of Power System Dominant Inter-Area Oscillation Paths

Yuwa Chompoobutrgool, *Student Member, IEEE*, and Luigi Vanfretti, *Member, IEEE*

***Abstract*—This paper presents three algorithms for identification of dominant inter-area oscillation paths: a series of interconnected corridors in which the highest content of the inter-area modes propagates through. The algorithms are developed to treat different sets of data: 1) known system model; 2) transient; and 3) ambient measurements from phasor measurement units (PMUs). These algorithms take feasibility into consideration by associating the network variables made available by PMUs, i.e., voltage and current phasors. All algorithms are demonstrated and implemented on a conceptualized Nordic Grid model. The results and comparison among three algorithms are provided. The applications of the algorithms not only facilitate in revealing critical corridors which are mostly stressed but also help in indicating relevant feedback input signals and inputs to mode meters which can be determined from the properties of dominant paths.**

***Index Terms*—Inter-area oscillations, network modeshapes, dominant path, power oscillation monitoring.**

I. Introduction

ONE goal of wide-area measurement system (WAMS) is to have tracking tools for oscillatory dynamics in interconnected power grids, particularly those which are critical to operational reliability, i.e., inter-area oscillations [1]. Insufficient damping of low-frequency inter-area oscillations arises as weak interconnected power systems are stressed to meet up with increasing demand [2]. This inadequacy may lead to oscillatory instability where the system can collapse.

"Interaction paths," which are defined as the group of transmission lines, buses, and controllers which the generators in a system use for exchanging energy during swings, are one important source of dynamic information necessary for WAMS [1]. If the interaction paths of inter-area swings can be identified, monitored, and tracked, proper preventive measures or control actions can be carried out to enhance the system's transfer capacity while maintaining high security.

An important characteristic of power oscillations is that, for every mode of oscillation, there exists a series of connecting corridors in which the highest content of the mode propagates through. For a particular case of inter-area modes, the path is termed "dominant inter-area oscillation path" [3], which is a concept based on the notion of interaction paths. These dominant inter-area oscillation paths are deterministic [4]. Furthermore, signals from the dominant path are the most observable and have the highest content of inter-area modes. Results from the study suggest that using the dominant path signals for wide-area control, adequate damping performance can be achieved.

The aim of this study is thus to propose and demonstrate a set of algorithms used to identify the critical interfaces which constrain power transfer capacity, namely dominant inter-area oscillation paths. Three algorithms are developed to treat different sets of information: 1) known system model; 2) transient; and 3) ambient measurements from phasor measurement units (PMUs). In particular, all of the algorithms employ voltage and current variables since they are practically available from PMUs. The outcomes of this study can be used to indicate critical corridors of inter-area oscillations and to select plausible feedback input signals to damping controllers.

This paper is organized as follows. Section II describes concepts and theories used in the study. The model-based algorithm and its demonstration on a test system is described in Section III. Section IV presents two algorithms for handling the two types of measurements from PMUs: transient and ambient data. Their corresponding algorithm demonstrations on the test system are provided. Algorithms comparison and important issues are discussed in Section V. Finally, the conclusions of this study are drawn in Section VI.

II. Theoretical Background

A. Power System Linearized Model

The linearized model of an N-machine power system can be given in a state-space form as

$$\begin{aligned}\Delta\dot{x}_P &= A_P\Delta x_P + B_P\Delta u_P\\ \Delta y_P &= C_P\Delta x_P + D_P\Delta u_P\end{aligned} \tag{1}$$

where A_P is the system matrix, B_P is the input matrix, C_P is the output matrix, D_P is the feedforward matrix, x_P is the state vector, u_P is the control vector, and y_P is the output vector.

Assuming $u_P = 0$, the model is expressed as

$$\underbrace{\begin{bmatrix}\Delta\dot{\delta}\\ \Delta\dot{\omega}\\ \Delta\dot{z}\end{bmatrix}}_{\Delta\dot{x}} = \underbrace{\begin{bmatrix}A_{11} & A_{12} & A_{13}\\ A_{21} & A_{22} & A_{23}\\ A_{31} & A_{32} & A_{33}\end{bmatrix}}_{A}\underbrace{\begin{bmatrix}\Delta\delta\\ \Delta\omega\\ \Delta z\end{bmatrix}}_{\Delta x} \tag{2}$$

where matrix A represents the state matrix corresponding to the state variables $\Delta\delta, \Delta\omega$, and Δz. Elements in z refer to other

Manuscript received May 25, 2012; revised September 17, 2012, October 25, 2012, November 03, 2012; accepted November 04, 2012. Date of publication December 24, 2012; date of current version July 18, 2013. The work of L. Vanfretti was supported by the STandUP *for* Energy collaboration initiative, Nordic Energy Research through the STRONg^2*rid* project and the European Commission through the *i*Tesla FP7 project. The work of Y. Chompoobutrgool was supported by Elforsk, Sweden. Paper no. TPWRS-00566-2012.

The authors are with the KTH Royal Institute of Technology, 100-44 Stockholm, Sweden (e-mail: luigiv@kth.se).

Color versions of one or more of the figures in this paper are available online at http://ieeexplore.ieee.org.

Digital Object Identifier 10.1109/TPWRS.2012.2227840

state variables. Then, performing eigenanalysis, the mode shape is derived from

$$A\Phi = \lambda\Phi \tag{3}$$

where λ are eigenvalues of the system and $\Phi = [\Phi_1 \Phi_2 \cdots \Phi_n]$ are the corresponding right eigenvectors (or mode shapes) and n is the number of state variables. Inter-area oscillations, as well as other modes, are determined from the eigenvalues.

B. Network Sensitivities [5]

The sensitivities of interest are those from network variables; namely, bus voltages and line current with respect to change in the state variables, e.g., machine's rotor angle (δ) or speed (ω). Since PMUs provide measurements in phasor form, the analyses in this study focus on two quantities: magnitude and angle. That is, the network sensitivities are the C_P matrix from (1) with voltage and current (both in magnitude and angle) as the outputs Δy. Voltage magnitude and angle are represented by V and θ, respectively, whereas line current magnitude are represented by I.

Sensitivities of the voltage magnitude (C_V) and angle (C_θ) are expressed as

$$\underbrace{\begin{bmatrix}\Delta V\\ \Delta\theta\end{bmatrix}}_{\Delta y} = \underbrace{\begin{bmatrix}\frac{\partial V}{\partial\delta} & \frac{\partial V}{\partial\omega} & \frac{\partial V}{\partial z}\\ \frac{\partial\theta}{\partial\delta} & \frac{\partial\theta}{\partial\omega} & \frac{\partial\theta}{\partial z}\end{bmatrix}}_{C} \underbrace{\begin{bmatrix}\Delta\delta\\ \Delta\omega\\ \Delta z\end{bmatrix}}_{\Delta x} = \begin{bmatrix}C_V\\ C_\theta\end{bmatrix}\begin{bmatrix}\Delta\delta\\ \Delta\omega\\ \Delta z\end{bmatrix}$$
$$C_V = [C_{V\delta} \quad C_{V\omega} \quad C_{Vz}]$$
$$C_\theta = [C_{\theta\delta} \quad C_{\theta\omega} \quad C_{\theta z}]. \tag{4}$$

In the same manner, sensitivity of the line current magnitude $(C_{I_{ft}})$ is expressed as

$$C_{I_{ft}} = \begin{bmatrix}C_{I_{ft}\delta} & C_{I_{ft}\omega} & C_{I_{ft}z}\end{bmatrix} \tag{5}$$

where the subscript ft indicates the direction of current from bus f to bus t.

C. Network Modeshape

As introduced in [5], network modeshapes (S) are the projection of the network sensitivities onto the modeshape, and are computed from the product of network sensitivities and mode shapes. They indicate how much of the content (open-loop observability) of each mode is distributed within the network variables. The expressions for voltage magnitude and angle modeshapes (S_V and S_θ) are

$$S_V = C_V\Phi, \quad S_\theta = C_\theta\Phi. \tag{6}$$

Similarly, for the line current magnitude we have

$$S_{I_{ft}} = C_{I_{ft}}\Phi. \tag{7}$$

The concept of network modeshape is used to characterize dominant paths for each mode of oscillation. Since the modes of concern in this study are those related to inter-area oscillations, the paths to be identified are those belonging to inter-area swings, hence, *dominant inter-area oscillation paths*.

Fig. 1. Conceptualization of the dominant path in a two-area system.

Dominant inter-area oscillation paths are defined as the passageway containing the highest content of the inter-area oscillations. For inter-area oscillations, current magnitude modeshapes $(S_{I_{ft}})$ indicate how much of the contents of the inter-area modes are distributed among the transfer corridors. Thus, for particular inter-area oscillations, corridors having the highest content of current magnitude modeshapes signify the paths where the inter-area oscillations will travel to the most. On the other hand, the magnitude of voltage magnitude and angle modeshapes (S_V and S_θ) indicate the modal observability of a signal. The larger in magnitude the modeshape is, the more observable the signal measured (from the dominant path) becomes. This will be helpful when selecting feedback signals having high inter-area modal contents.

D. Dominant Inter-Area Oscillation Paths

Consider a conceptualized two-area system shown in Fig. 1, G_1 and G_2 represent the main clusters of machines involved in the inter-area swing while transformers and line impedances represent elements of the dominant path connecting the two areas.

Characteristics of dominant inter-area paths[1] can be demonstrated using the computed voltage magnitude (S_V) and angle modeshapes (S_θ) as illustrated in Fig. 2(a) and (b), respectively. Fig. 2(c) and (d) illustrate the corresponding magnitude $(|S_\theta|)$ and phase $(\angle S_\theta)$ of the voltage angle modeshapes, S_θ. Two loading cases, Case 1 having the power transfer of 1100 MW and Case 2 having the power transfer of 900 MW, are compared in this figure. From the figure, Case 1 and Case 2 are denoted in blue and red, respectively. The x-axis represents the bus number in the dominant path; the distance between buses are proportional to the line impedance magnitude. According to the figure, important features of the dominant path are summarized here.

- The smallest $|S_\theta|$ element(s) [Fig. 2(c)] or the largest S_V [Fig. 2(a)] indicates the center of the path. This center can be theorized as the "inter-area mode center of inertia" or the "inter-area pivot" that exists for each of the system's inter-area modes.
- The pivot divides the path into two groups where their respective phases are opposing each other [Fig. 2(d)].
- The difference between S_θ elements of two edges of the path [Fig. 2(b)] are the largest among any other pair within the same path. In other words, the oscillations are the most

[1]These are similar to the characteristics of voltage change and angle change of the first swing mode in Fig. 13 [6] where the mode is described by a single wave equation with one spatial dimension.

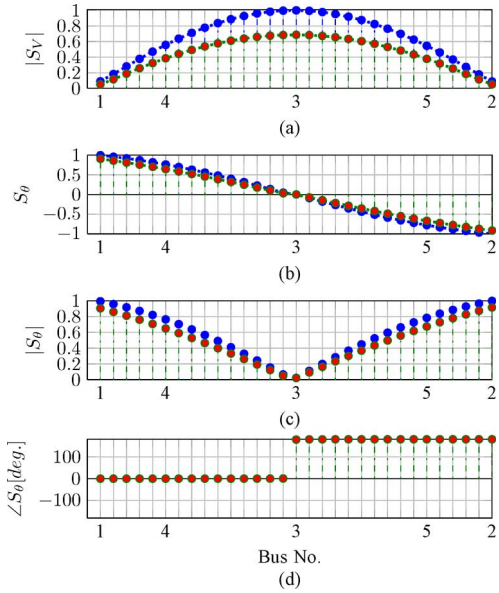

Fig. 2. Voltage magnitude and angle modeshapes of the dominant path in the two-area system. (a) Magnitude of voltage magnitude modeshape. (b) Voltage angle modeshape. (c) Magnitude of voltage angle modeshape. (d) Angle of voltage angle modeshape.

positive at one end while being the most negative at the other end. Hence, they can be theorized as the "tails" for each inter-area mode.

- S_V elements of the edges [Fig. 2(a)] are the smallest or one of the smallest within the path.
- Inter-area contents of the voltage magnitude modeshapes are more observable in a more stressed system.

As previously stated, the dominant path of any mode of oscillation, particularly in this study those of inter-area modes, can be identified by means of network modeshape computations. An algorithm to carry out this task is presented next.

III. Model-Based Algorithm

To identify dominant inter-area oscillation paths for a known system model, the following algorithm is proposed.

Step 1) Solve the power flow of the original system and determine the initial conditions of all network variables.

Step 2) Perform linearization. Obtain the network sensitivities matrices C_V, C_θ, and $C_{I_{ft}}$ from (4) and (5).

Step 3) Perform eigenanalysis to obtain mode shapes (Φ) from (3) and identify the inter-area modes; the modes having lowest damping ratios are the ones of concern.

Step 4) Compute the network modeshapes corresponding to the inter-area modes: $S_{V,i}$, $S_{\theta,i}$, and $S_{I_{ft},i}$. (Note: i refers to ith mode).

Step 5) Sort the current magnitude modeshapes in descending order. Identify the lines and their corresponding sending and receiving buses for the sorted modeshape.

Step 6) The dominant path is determined from the lines having highest content of current magnitude modeshapes, $S_{I_{ft},i}$. Compare with the schematic diagram of the system of study and identify the path.

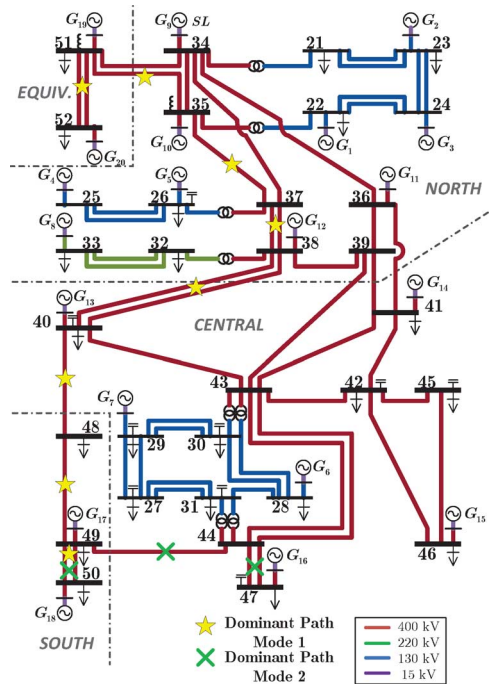

Fig. 3. KTH-NORDIC32 System.

Step 7) Verify the characteristics of the path using its corresponding voltage magnitude and angle modeshapes. The results should resemble the dominant inter-area oscillation path's features shown in Fig. 2.

A. Algorithm Demonstration Using the KTH-NORDIC32 System

The system under study, namely KTH-NORDIC32 [7] (illustrated in Fig. 3), is a conceptualization of the Swedish power system and its neighbors. It has 20 generators and 52 transmission lines (see Table I for generator dispatch). Small-signal stability analysis reveals that the system has two lightly damped low frequency inter-area oscillations: 0.50 and 0.74 Hz. Note that, to develop a fundamental understanding, we consider a case where controls such as exciters and turbine governors are neglected.[2] Two loading scenarios, namely Case 1 and Case 2, are used to illustrate the algorithm throughout this study. Power flow from the northern to the southern regions for each respective scenario are 3 134 and 2 933 MW. Note that the step-by-step demonstration will be described only for Case 1 loading scenario.

Steps 1)–3) After solving the power flow, performing linearization, and applying eigenanalysis to the linearized model of the KTH-NORDIC32 system, the two main electromechanical modes having lowest damping ratios are 0.50 Hz (Mode 1) and 0.74 Hz (Mode 2). Mode 1 denotes the swing between groups of machines in the north and equivalent regions against those in the central and south regions, whereas Mode 2 denotes the swing between groups of south machines against those of

[2]The model with controls is studied in [7]. The controls have, to some extent, impact on the magnitude of network modeshape. However, the inter-area oscillations have a strong correlation with the machine swing equation [8] and, thus, are largely determined by generator rotor angle and speed. Therefore, classical models are used in this study.

TABLE I
GENERATOR DISPATCH

Generator	Power Rating (MVA)	Generator	Power Rating (MVA)
G_1	800	G_{11}	300
G_2	600	G_{12}	350
G_3	700	G_{13}	300
G_4	600	G_{14}	700
G_5	250	G_{15}	1200
G_6	400	G_{16}	700
G_7	200	G_{17}	600
G_8	850	G_{18}	1600
G_9	1000	G_{19}	500
G_{10}	800	G_{20}	4500

TABLE II
TEN LARGEST LINE CURRENT MAGNITUDE MODESHAPES OF MODE 1

Sending Bus, f	Receiving Bus t	$S_{I_{ft},1}$
18	50	3.50
40	48	2.96
48	49	2.19
44	49	1.91
49	50	1.79
49	50	1.79
37	38	1.31
37	38	1.31
38	40	1.31
38	40	1.31

the central area. Since the algorithm is applicable to any swing mode, the following steps will be illustrated in detail for Mode 1's dominant inter-area path.

Step 4) Compute network modeshapes corresponding to Mode 1: $S_{V,1}$, $S_{\theta,1}$, and $S_{I_{ft},1}$.

Step 5) Sort $S_{I_{ft},1}$ in descending order. The ten largest line current modeshapes and their corresponding sending and receiving buses are described in Table II.

Step 6) The dominant inter-area oscillation path for Mode 1 is identified to be comprised by the corridor 52-51-35-37-38-40-48-49-50 (considering only high-voltage nodes).

Step 7) Voltage magnitude and angle modeshapes of the dominant path are constructed to justify the dominant path in Fig. 4. Note that network modeshapes are normalized. Before obtaining Fig. 4(b), the pivot of the path can be obtained from the minimum of $|S_\theta|$ from Fig. 4(c) which corresponds to the midpoint of $\angle S_\theta$ in Fig. 4(d), Bus 37. This pivot is used as the reference in plotting angle modeshapes. The comparison between two loading cases are illustrated in Fig. 5(a) where blue and green dots represent Case 1 and Case 2, respectively. Note that the main features of the dominant paths remain preserved. Thus, the dominant path of Mode 1 is justified. Note that intermediate points between buses are fictitious modes and used only for the purpose of illustration.

Repeating Steps 4)–7) for Mode 2, the dominant inter-area oscillation path for Mode 2 is identified to be the corridor 50-49-44-47. Voltage magnitude and angle modeshapes of the path for both cases are illustrated in Fig. 5(b). Similar to Mode 1, the main features of the dominant paths remain preserved and, thus, the path is justified.

Comparing the two loading cases in Mode 1 [Fig. 5(a)], it can be seen that S_V of Case 2 is shifted leftwards; the modal content

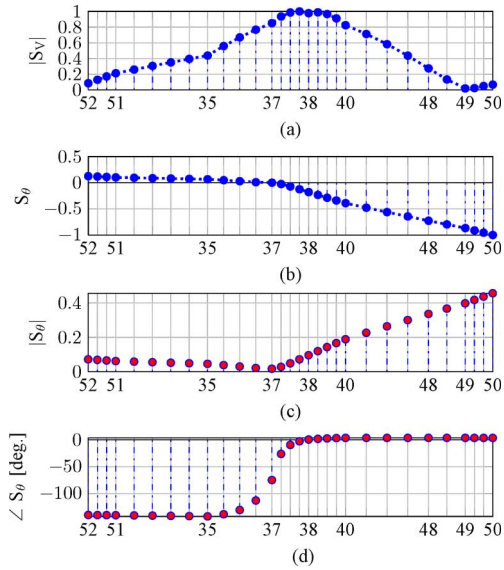

Fig. 4. Voltage magnitude and angle modeshapes of Mode 1, Case 1. (a) Magnitude of voltage magnitude modeshape. (b) Voltage angle modeshape. (c) Magnitude of voltage angle modeshape. (d) Angle of voltage angle modeshape.

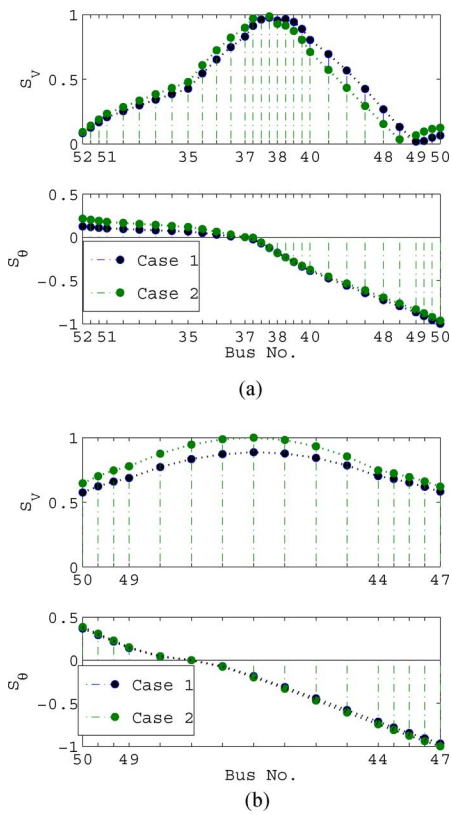

Fig. 5. Dominant inter-area oscillation path, model-based algorithm. (a) Mode 1. (b) Mode 2.

of Mode 1 is higher on the left-hand path while lesser on the right-hand path. This is the effect of higher loading through the path. S_θ of Case 2 marginally shifts but maintains mounting on the same pivot as that of Case 1.

Although both cases have a similar amount of Mode 1 contents, the loading condition of Case 2 excites the modal content of Mode 2 more than Case 1. This can be observed from

Fig. 5(b), where S_V of Case 2 is higher than that of Case 1. Again, this is the effect of loading.

This result, however, may not always be the case with other loadings since the dominant paths may be subject to changes depending on system's operating conditions.

IV. Measurement-Based Algorithms

The model-based algorithm utilizes a linearized power system model and, thus, is applicable and justified only for specific operating points upon which the system has been linearized. Since real power systems are not linear and subject to different operating points, the linearized model of the power system may not always be accurate (or available). It is, thus, more sensible to employ measurements. Measurements from phasor measurement units (PMU) contain "actual" system modes and can capture the nonlinear response of the system. As such, an algorithm that takes into account these considerations is necessary.

Here, two algorithms are developed for disposing of two types of measurement data: transient and ambient. For measurements of transient events, time-domain simulated signals can be considered as synthetic measurements from PMUs, making the approach applicable using synchrophasors. This can be simulated by implementing a perturbation that results in measurements from which not only the linear operating regime of the power system can be extracted, but also the dominant electromechanical oscillations should be excited in the synthesized signals. This synthetic data is used as if it had originated from actual PMUs.

The step-by-step algorithm for transient measurement is described below.

A. Algorithm for Transient Measurements

Step 1) Obtain synchronized phasor measurements which contain the dynamic response of the power system in its linear operating regime, i.e., "ringdown measurements" [9].

Step 2) Compute the deviations in line current magnitude (ΔI_{ft}), voltage magnitude (ΔV) and voltage angle $(\Delta\theta)$.

Step 3) Apply any modal identification algorithm to ΔI_{ft} measurements to identify dominating modes, i.e., poorly damped low frequency inter-area oscillations.

Step 4) Filter ΔI_{ft} measurements such that only selected dominant inter-area modal content is preserved in the signals.

Step 5) Select an appropriate window of data. Find the largest absolute value for each filtered ΔI_{ft} measurement within the selected window, and sort the measurements in descending order.

Step 6) The dominant inter-area oscillation path is determined from the lines having largest content of the filtered ΔI_{ft} signals. Compare to the schematic diagram of the system of study and identify such path.

Step 7) Verify the characteristics of the dominant path using its corresponding voltage magnitude and angle deviations: ΔV, and $\Delta\theta$. The results should resemble the dominant inter-area oscillation path's features shown in Fig. 2.

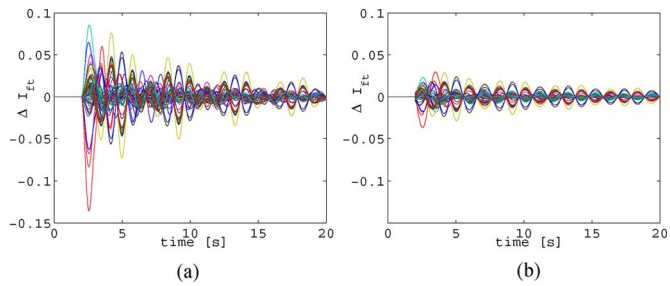

Fig. 6. ΔI_{ft} responses after a small perturbation, KTH-NORDIC32 system. (a) Before filtering. (b) After filtering.

B. Algorithm Demonstration Using the KTH-NORDIC32 System

Using the same test system, the transient measurement-based algorithm is applied to the synthetic data from simulations of the KTH-NORDIC32 system in this section. Note that only loading Case 1 will be illustrated.

Step 1) PMU measurements are synthesized by applying a small disturbance to the test system to excite its dynamics. A perturbation of 0.1 p.u. is applied at the mechanical power of G_{15} at $t = 2$ s for 1 s and the system is simulated for 20 s.

Step 2) Compute ΔI_{ft}. Responses of ΔI_{ft} are shown in Fig. 6.

Step 3) Eigensystem realization algorithm (ERA) [10]–[13][3] is a technique employed to identify oscillatory components in each measurement. The ERA is applied to the change in line current magnitude measurements ΔI_{ft}. Two main oscillatory modes having the lowest damping ratios are 0.49 Hz (Mode 1) and 0.72 Hz (Mode 2), respectively. The following steps will be illustrated only for the dominant inter-area path of Mode 1.

Step 4) Filters are used to screen out frequency components so that only the content of Mode 1 remains. The filtered ΔI_{ft} are obtained as shown in Fig. 6(b).

Step 5) The selected window of the filtered ΔI_{ft} is displayed in Fig. 7. The largest absolute value for each measurement is sorted in descending order; the ten largest value and their corresponding sending and receiving buses are summarized in Table III.

Step 6) Similar to the model-based algorithm, the dominant inter-area oscillation path for Mode 1 is identified to be 52-51-35-37-38-40-48-49-50.

[3]Details of the ERA algorithm with examples for power system applications are provided in this reference.

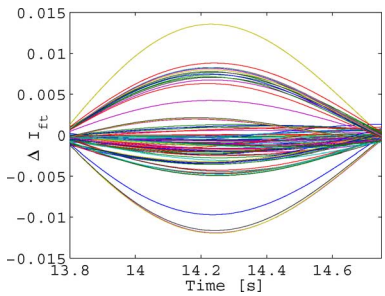

Fig. 7. Selected window of I_{ft}.

TABLE III
TEN LARGEST LINE CURRENT DEVIATIONS OF MODE 1

Sending Bus, f	Receiving Bus t	$\lvert\Delta I_{ft,1}\rvert \times 10^{-2}$
18	50	1.54
48	49	0.98
44	49	0.94
49	50	0.83
49	50	0.83
40	48	0.72
17	49	0.48
20	52	0.33
37	38	0.33
37	38	0.33

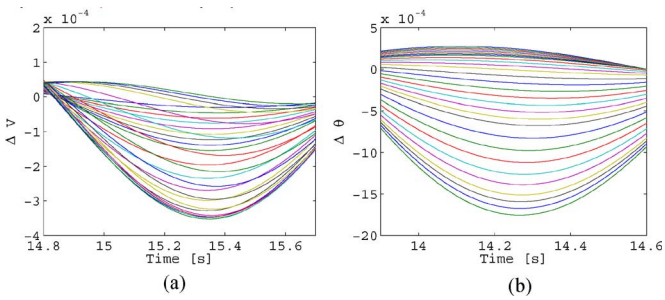

Fig. 8. Selected windows of voltage magnitude and angle deviation of the dominant path for Mode 1. (a) Voltage magnitude deviations. (b) Voltage angle deviations.

Step 7) Applying the same filters to ΔV and $\Delta\theta$ of the buses on the dominant path, appropriate windows are selected separately for each type of signal.[4] The selected windows for voltage magnitude and angle deviations are illustrated in Fig. 8(a)–(b), respectively.

The largest absolute value for each measurement on Mode 1's dominant path are used to construct voltage magnitude and angle deviations plots of the path as illustrated in Fig. 9(a), where blue and green dots represent loadings of Case 1 and Case 2, respectively.

From the figure, Case 1 has larger modal content in ΔV from the pivot to the right-hand side of the path (with an exception for Bus 49 and 50) whereas, mounting on the same pivot in both cases, $\Delta\theta$ marginally shifts. Furthermore, the resulting differences between the two edges of both cases are comparable.

[4]For all of the network variables, the independent modal components do not peak at the same instants [12].

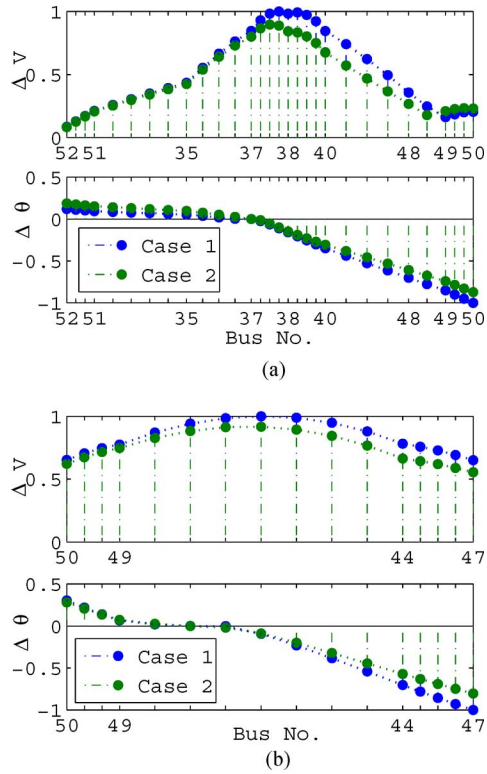

Fig. 9. Dominant inter-area oscillation paths, transient measurements. (a) Mode 1. (b) Mode 2.

Repeating *Steps 4)–7)* for Mode 2, the dominant inter-area oscillation path for Mode 2 is identified to be 50-49-44-47. Voltage magnitude and angle deviations of the path are illustrated in Fig. 9(b). Similar to the result from Mode 1, Case 1 has larger modal content in ΔV.

Comparing with Fig. 2, the main features of the dominant paths remain preserved. Thus, the dominant paths of both modes are justified.

Note that with transient data, changes in voltage magnitude and angle modeshapes on dominant inter-area mode paths for different operating conditions depend on disturbance locations, which mode(s) is excited and how much it is excited.

C. Algorithm for Ambient Measurements

Ambient measurements are synthesized by simulating the time response of the power system with random white noise[5] and small step inputs at all loads [14]. The algorithm for handling ambient measurements is described here.

Step 1) Preprocess a parcel of ambient measurements ΔI_{ft}, ΔV, and $\Delta\theta$ by filtering all of the measurements such that only inter-area modal content of interest is preserved in the signals.

Step 2) Compute the power spectral density (PSD) of ΔI_{ft}.

Step 3) Select an appropriate window. Find the peak PSD for each signal within the selected window and sort the contents in descending order.

Step 4) The dominant inter-area oscillation path is determined from the signals having largest PSD contents.

[5]Uniformly distributed pseudorandom values are drawn from the standard uniform distribution using MATLAB's `rand` function.

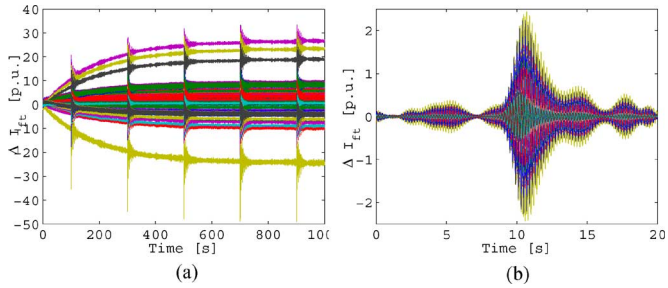

Fig. 10. $\Delta I_{\rm ft}$ signals before and after preprocessing. (a) Before preprocessing. (b) After preprocessing, (from 0 to 20 s).

Compare with the schematic diagram of the system of study and identify such path.

Step 5) Using one of the edges as a reference, cross power spectral density (CPSD) of the preprocessed ΔV, and $\Delta\theta$ of the dominant path are computed.

Step 6) Select appropriate windows for each type of signal. Find the corresponding largest CPSD magnitude for each measurement within the selected window.

Step 7) Verify the characteristics of the dominant path using its corresponding peak CPSD of voltage magnitude and angle. The results should resemble the dominant inter-area oscillation path's features shown in Fig. 2.

D. Algorithm Demonstration Using the KTH-NORDIC32 System

Step 1) $\Delta I_{\rm ft}$ measurements before and after preprocessing are illustrated in Fig. 10.

Step 2) The computed PSD of $\Delta I_{\rm ft}$ are illustrated in Fig. 11. The dashed red lines indicate the cutoff frequencies used in preprocessing.

Steps 3) The peak PSD for each $\Delta I_{\rm ft}$ is sorted in descending order; the ten largest values and their corresponding sending and receiving buses are summarized in Table IV.

Step 4) The dominant inter-area oscillation path for Mode 1 is identified to be 52-51-35-37-38-40-48-49-50.[6]

Step 5) ΔV_{52} and $\Delta\theta_{52}$ are used as references for CPSD computation of voltage magnitude and voltage angle measurements of the dominant path, respectively. The corresponding computed CPSD are illustrated in Fig. 12.

Step 6) After selecting appropriate windows, the largest (absolute) CPSD values for each measurement within the dominant path are used to reconstruct the path. Using the characteristics of the dominant path from Fig. 2(c)–(d), the bus having the smallest magnitude of voltage angle deviations, $|\Delta\theta|$, is the pivot of the path and thus used as the reference. The reconstructed dominant path of Mode 1 is as shown in Fig. 13(a) with blue dots for Case 1.

Step 7) The characteristics of the obtained path are verified by comparing them with Fig. 2. The main features of the dominant paths remain preserved, and, thus, the path is justified.

[6]Observe from Table IV that the path 42-43-44-49-50 has considerably high content of Mode 1, however, it has lesser content than that of the specified dominant path. This second path is thus termed "secondary dominant inter-area oscillation path".

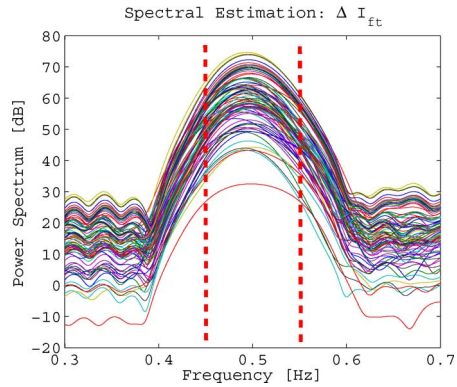

Fig. 11. PSD of $\Delta I_{\rm ft}$, Mode 1.

TABLE IV
TEN LARGEST PSDS OF $\Delta I_{\rm ft}$

Sending Bus, f	Receiving Bus t	PSD [dB]
18	50	74.69
40	48	74.14
48	49	71.35
44	49	70.81
49	50	69.77
49	50	69.77
42	43	67.68
43	44	66.60
43	44	66.60
38	40	66.46

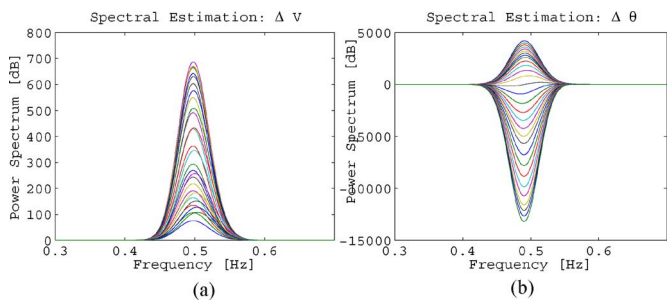

Fig. 12. Computed CSD of the dominant path. (a) Voltage magnitude. (b) Voltage angle.

Comparing the two loading case studies in Fig. 13(a), Case 1 has overall larger modal content in ΔV while $\Delta\theta$ marginally shifts, but are about the same in both cases. The differences between the two edges of both cases are comparable.

Repeating *Steps 1)–7)* for Mode 2, the dominant inter-area oscillation path for Mode 2 is identified to be 50-49-44-47. Voltage magnitude and angle deviations of the path are illustrated in Fig. 13(b). Similar to the result from Mode 1, Case 1 has larger modal content in ΔV.

V. DISCUSSION

A. Algorithms Comparison

Ideally, if all of the parameters and exact model of the system are known, one can promptly use the model-based algorithm. However, this is difficult in practice, and, thus, measurements (from synchrophasors) can be used as the primary source of information. The use of the model-based algorithm could be

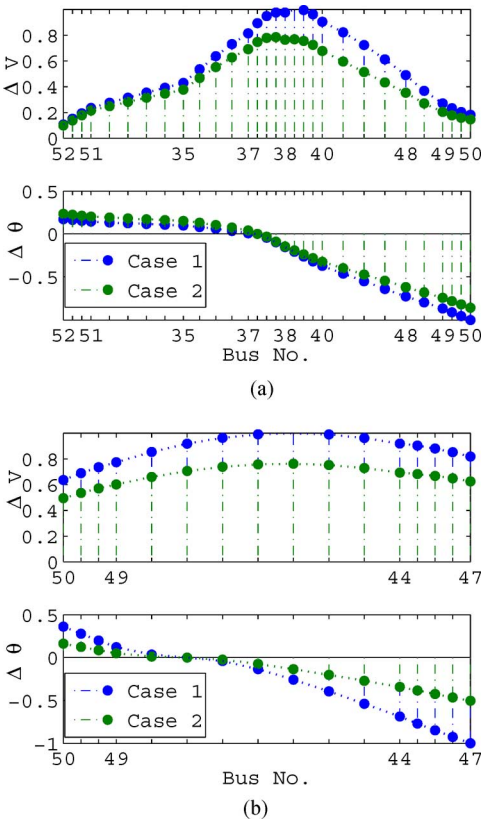

Fig. 13. Dominant inter-area oscillation paths, ambient measurements. (a) Mode 1. (b) Mode 2.

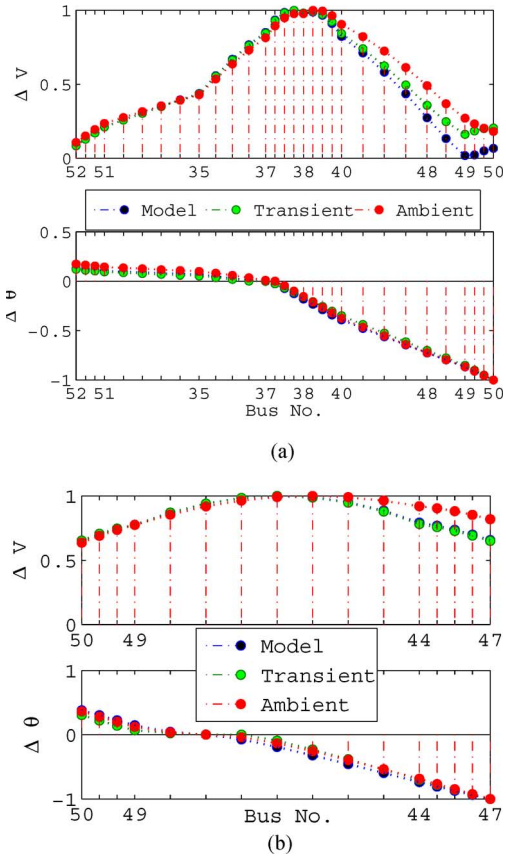

Fig. 14. Comparison among the three algorithms, loading Case 1. (a) Mode 1. (b) Mode 2.

more adequate for planning studies (for example, PMU placement analysis) and postmortem analysis for enhancing dynamic models.

To verify the performance of the measurement-based algorithms, their results are compared with that of the model-based algorithm as illustrated in Fig. 14. Overall, the three algorithms share the same general properties of the dominant inter-area oscillation paths with close matching. Nevertheless, one-to-one match should not be expected since the two types of measurement data have different features; the disturbance in transient simulations can excite dynamics of a particular mode more or less to what can be observable in the ambient measurement data.

For all of the algorithms, the results of voltage angle deviation, sharing the same pivot, are resembling whereas those of voltage magnitude deviation slightly differ. These differences are possibly due to several factors of which the more influential ones are expected to be: 1) loading; 2) types, magnitudes, and locations of disturbances; or 3) locations of loads. Additional research is being performed to answer to these issues.

Observe that Bus 49 and Bus 50 are parts of both dominant paths. Hence, they can be good candidates for feedback input signals for damping control design when considering multiple modes.

B. Challenges and Limitations of the Algorithms Working With Measurements

1) Reference Selection: For voltage angle measurements, a reference is required. Consequently, plots of $\Delta\theta$ on the dominant inter-area path depend on which reference is chosen. The proposed algorithms systematically specify which reference to be chosen. If an arbitrary signal were chosen as a reference, this would certainly change the resulting angle differences. An example of different reference signals on the $\Delta\theta$ of the dominant inter-area path of Mode 1 is illustrated in Fig. 15 where blue, green and red dots represent the pivot, Bus 52, and Bus 50 as the reference signals, respectively.

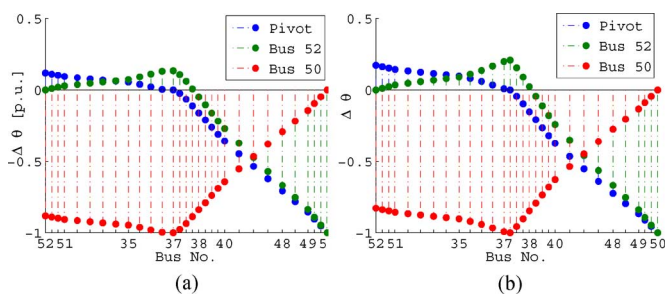

Fig. 15. Impact of different reference signals on the measurement-based algorithms. (a) Transient measurements. (b) Ambient measurements.

2) Window Selection: For the algorithm using transient measurements, a window of data must be selected in such a way that the measurements contain only the "ringdown" of the responses [13]. This means that, to perform satisfactorily, the algorithm requires that the small signal dynamics are excited. This is actually a general problem of window selection for inter-area mode identification algorithms discussed in [13]. In addition, after *Step 4)*,

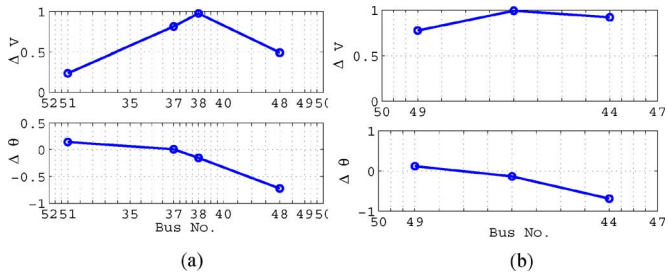

Fig. 16. Dominant inter-area oscillation paths, scarce measurement case. (a) Mode 1. (b) Mode 2.

care must be taken so that the window selected contains only half cycle of the oscillation for which the filter was designed (inter-area mode frequency). For the algorithm using ambient data, note that it is meant to be continuously applied. A rolling window of 20 s was used in this study. In practice, this window can have an overlap of 50% as required by nonparametric estimators such as Welch [14].

3) Abundant Versus Scarce Measurements: With abundant measurements, one can determine the dominant paths using the algorithms above and choose signals from them to monitor the inter-area modes and/or to provide feedback signals for damping controllers. However, at present, PMUs are not yet available everywhere in power systems, and it would be unreasonable to assume this will be the case in the near future. Hence, if only the available signals were to be used, the algorithms could help determining (although partially) dominant paths or at least help in highlighting those signals with the highest possible content of inter-area modes. Although those available signals may not contain the theoretically highest inter-area modal contents, they give the "practically" highest modal contents available.

In the preceding section, the measurements were assumed to be available at all high voltage buses. To illustrate a case of scarce measurements, it is assumed that only the following measurements are available: buses 51, 37, 38, and 48 (see Fig. 9(a) for Mode 1), and buses 49, 44, and a fictitious bus lying in the middle of the path [see Fig. 9(b)] for Mode 2. Using these measurements, the dominant paths are reconstructed as shown in Fig. 16. With certain measurements availability, a dominant path of a mode of concern can be reconstructed. However, this is dependent on the system and no general conclusion can be drawn. For any relevant PMU placement methodology, small signal observability theory needs to be further developed. The results in this article, [5] and [3] could be used to develop such algorithm.

C. Considerations for Implementation

It is to be emphasized that *Step 4)* in "Algorithm for Transient Measurements" is crucial. The selected frequencies for filtering can help in isolating the modal content from the inter-area mode, and thus the resulting signals will have consistent frequency content at only a narrow frequency range close to the inter-area mode. Note that when oscillations occur through the high-voltage (HV) network, this effect will be noticed through all of the HV buses in both the voltage magnitude and angle, see [15]. As a consequence, in one cycle of the oscillation under normal damping conditions (5%–15% damping), the effect of damping will actually drive the decay *throughout* all of the network variables (supporting theory illustrated in [5]).

In the case of growing oscillations where the damping is changing rapidly (in the case of instability), the algorithm using transient (or ringdown) data is not adequate. As an example, consider the WECC 1996 system breakup [9]. There were only a few "ringdowns" to obtain mode estimates, i.e., data that could be presumably used by the algorithm using transient responses. In this case the ringdowns would have been sufficient to detect the topology changes and to determine a *new* dominant path product of the loss of critical lines. However, this data would have been insufficient to detect the same topology changes continuously and quickly enough. The continuous reduction of damping is actually an indicator that the dominant path is changing. It is important then to "track" how the main interfaces are being modified by increased grid stress. In view of the above, the algorithm using ambient data, which allows for continuous monitoring, is proposed. For any actual implementation, the ambient data algorithm should be preferred, using the algorithm depending on "transient" data only to cross validate the results of the ambient data algorithm when ringdowns become available in the network.

If a "dominant path tracing" application were to be implemented in a control room, such application should automatically adapt to the primary data available. In other words, the application should primarily work using ambient measurements, and cross validate its results when a transient becomes available. An implementation of such application should make the identification of the dominant path and algorithm selection completely transparent to the user, and, moreover, with self-validation tools using different algorithms to verify results of each other. To further elaborate the actual implementation, the following schemes are proposed for each type of data as follows:

Ambient data: the algorithm runs continuously, using a rolling window of 20 s of data with 50% overlap. Note that the size of the rolling window could be reduced by properly tuning the parameters of nonparametric spectral estimators. This window size is selected assuming that any relevant topology changes capable of modifying the "dominant path" would be detected within the rolling window.

Transient (ringdown) data: this algorithm requires a ringdown to be present in the data. Thus, it is suitable to use it for validation of the results from ambient data when topology changes occur. Moreover, if the available ambient data suffers from insufficient spectral content, this application can instead be used to compute the dominant path.

Model: it would be needed that the dynamic model is available from a dynamic security assessment (DSA) tool and properly updated. This means that the positive sequence dynamic model has to be updated from the last snapshot of the energy management systems (EMS) with the most recent topology changes included, and its dynamics initialized considering the steady state solution of this EMS update. However, the issue lies in how fast the updating of this dynamic model can be performed and the effort needed to carry out the related computations of the algorithm so that relevant information can be provided to the operator quickly enough. Considering these

limitations, this algorithm (being supplied by proper models from a DSA tool) is better suited as a tool for validation of the results from the ambient data and ringdown algorithms.

VI. Conclusion

This paper presents three types of algorithms, subject to different types of information, to identify dominant inter-area oscillation paths in interconnected power systems, regardless of scale. These algorithms are illustrated and justified using the KTH-NORDIC32 study system. The performance of the three algorithms are consistent with each other and in accordance with the main features of the ideal dominant path.

The dominant inter-area oscillation paths have the highest content of the inter-area modes; they are the tracks where the modes travel to the most and where the swing machines are located. These dominant paths can help in placing PMUs such that the modal content can be most observed. Furthermore, using signals from the dominant paths, it is anticipated that damping of the inter-area oscillations can be improved. This will be investigated in a further study.

References

[1] J. Hauer, D. Trudnowski, and J. DeSteese, "A perspective on WAMS analysis tools for tracking of oscillatory dynamics," in *Proc. IEEE Power and Energy Soc. General Meeting*, Tampa, FL, Jul. 2007, pp. 1–10.

[2] G. Rogers, "Demystifying power system oscillations," *IEEE Computer Applications in Power*, pp. 30–35, Jul. 1996.

[3] Y. Chompoobutrgool and L. Vanfretti, "On the persistence of dominant inter-area oscillation paths in large-scale power networks," in *Proc. 8th IFAC Symp. Power Plants and Power Syst.*, Toulouse, France, Sep. 2012, pp. 1–6.

[4] J. Hauer, W. Mittelstadt, K. Marting, J. Burns, and H. Lee, *Power System Stability and Control: The Electric Power Engineering Handbook*. Boca Raton, FL: CRC, 2007, ch. 14, pp. 14-1–14-52, Integrated Dynamic Information for the Western Power System: WAMS Analysis in 2005.

[5] L. Vanfretti and J. Chow, "Analysis of power system oscillations for developing synchrophasor data applications," in *Proc. IREP Symp. Bulk Power Syst. Dynamics and Control*, Rio de Janero, Brazil, Aug. 2010, pp. 1–17.

[6] R. Cresap and J. Hauer, "Emergence of a new swing mode in the western power system," *IEEE Transactions on Power Apparatus and Systems*, vol. PAS-100, no. 4, pp. 2037–2045, Apr. 1981.

[7] Y. Chompoobutrgool, W. Li, and L. Vanfretti, "Development and implementation of a nordic grid model for power system small-signal and transient stability studies in a free and open source software," in *Proc. IEEE Power and Energy Soc. General Meeting*, San Diego, CA, Jul. 2012, pp. 1–8.

[8] F. DeMello, P. Nolan, T. Laskowski, and J. Undrill, "Coordinated application of stabilizers in multimachine power systems," *IEEE Trans. Power App. Syst.*, vol. PAS-99, no. 3, pp. 892–901, May 1980.

[9] D. Trudnowski and J. Pierre, "Signal processing methods for estimating small-signal dynamic properties from measured responses," in *Inter-Area Oscillations in Power Systems: A Nonlinear and Nonstationary Perspective*. New York: Springer, 2009, pp. 1–36.

[10] J. Juang and R. Pappa, "An eigensystem realization algorithm for modal parameter identification and model reduction," *J. Guidance Control*, vol. 8, no. 5, pp. 620–627, 1985.

[11] J. Sanchez-Gasca, "Toward the automated computation of electromechanical modes from transient simulations," in *Proc. IEEE Power and Energy Soc. General Meeting*, Minneapolis, MN, Jul. 2010, pp. 1–7.

[12] L. Vanfretti and J. Chow, "Identification of dominant inter-area modes in the eastern interconnection from PMU data of the FRCC 2008 disturbance: An eigensystem realization algorithm illustration," in *Contribution to Special Publication of the Task Force on Modal Identification of Electromechanical Modes*. : IEEE PES, 2012 [Online]. Available: http://urn.kb.se/resolve?urn=urn:nbn:se:kth:diva-63377

[13] "IEEE PES task force on modal identification of electromechanical modes," *Identification of Electromechanical Modes in Power Systems* Jun. 2012 [Online]. Available: http://www.pes-store.org/p-13616.htm

[14] L. Vanfretti, S. Bengtsson, V. Aarstrand, and J. Gjerde, "Applications of spectral analysis techniques for estimating the nordic grid's low frequency electromechanical oscillations," in *Proc. 16th IFAC Symp. Syst. Identification*, Brussels, Belgium, Jul. 2012, pp. 1–6.

[15] J. Chow, L. Vanfretti, A. Armenia, S. Ghiocel, S. Sarawgi, N. Bhatt, D. Bertagnolli, M. Shukla, X. Luo, D. Ellis, D. Fan, M. Patel, A. Hunter, D. Barber, and G. Kobet, "Preliminary synchronized phasor data analysis of disturbance events in the us eastern interconnection," in *Proc. IEEE PES Power Syst. Conf. Exp.*, Mar. 2009, pp. 1–8.

Yuwa Chompoobutrgool (S'09) received the B.Sc. degree in electrical power engineering from Sirindhorn International Institute of Technology (SIIT), Thailand, in 2006, and the M.Sc. degree in energy science from Kyoto University, Kyoto, Japan, in 2009. She is currently working toward the Ph.D. degree at the School of Electrical Engineering, Electric Power Systems, KTH Royal Institute of Technology, Stockholm, Sweden.

Her research interests are stability and control of power systems, particularly wide-area damping control and system modelling.

Luigi Vanfretti (M'10) received the degree in electrical engineering from Universidad de San Carlos de Guatemala in 2005, and the M.Sc. and Ph.D. degrees in electric power engineering from Rensselaer Polytechnic Institute, Troy, NY, in 2007 and 2009, respectively.

He was a Visiting Researcher with The University of Glasgow, Scotland, in 2005. He became an Assistant Professor with the Electric Power Systems Department, KTH Royal Institute of Technology, Stockholm, Sweden, in 2010 and was conferred the Swedish title of "Docent" in 2012. His main research interest is on the development of PMU data-based applications.

Dr. Vanfretti has served, since 2009, in the IEEE PES PSDP Working Group on Power System Dynamic Measurements, where he is now Vice- Chair. In addition, since 2009, he has served as Vice-Chair of the IEEE PES CAMS Task Force on Open Source Software. He is an evangelist of Free/Libre and Open Source Software. For his research and teaching work towards his Ph.D. degree, he was awarded the Charles M. Close Award from Rensselaer Polytechnic Institute.